Suppression of quantum Hall plateaus and nonlinear Landau level fan diagram in a parabolic quantum well

K. Ensslin, M. Sundaram, Achim Wixforth, A.C. Gossard

Angaben zur Veröffentlichung / Publication details:

Ensslin, K., M. Sundaram, Achim Wixforth, and A.C. Gossard. 1992. "Suppression of quantum Hall plateaus and nonlinear Landau level fan diagram in a parabolic quantum well." *Surface Science* 267 (1-3): 553–57. https://doi.org/10.1016/0039-6028(92)91198-k.

Suppression of quantum Hall plateaus and nonlinear Landau level fan diagram in a parabolic quantum well

K. Ensslin [a,b], M. Sundaram [b], A. Wixforth [a] and A.C. Gossard [b]

[a] *Sekt. Physik, Univ. München, Geschw. Scholl Pl. 1, W-8000 München 22, Germany*
[b] *Materials Department, University of California, Santa Barbara, CA 93106, USA*

The Hall resistance of a parabolic quantum well reveals suppressed quantum Hall plateaus at even-integer filling factors. This phenomenon is explained by the particular subband structure of the investigated system, which leads to a nonlinear Landau level fan diagram in a magnetic field.

The integral quantum Hall effect is mostly studied in high mobility two-dimensional electron gases (2DEG) [1], where the extension of the wave function perpendicular to the 2DEG is typically ≈ 10 nm. The subband separation in these systems is much larger than the cyclotron energy $\hbar\omega_c$ for moderate magnetic fields ($B < 10$ T). Furthermore, if an upper subband is populated, its carrier density N_s^1 is much smaller (typically a factor of 10) than the carrier density N_s^0 of the ground subband.

In a parabolic quantum well (PBW) the situation is completely different. The extent of the wave function can cover more than 0.5 μm [2,3] leading to subband separations below 1 meV. The carrier densities of two neighboring subbands can be within a factor of two and, in a magnetic field, they can even coincide, i.e. they can have the same filling factor. This interesting situation can be realized in our samples by an independent tuning of the total carrier density N_s via a front gate voltage V_g and the subband densities via the magnetic field B. For low carrier densities in the upper subband $N_s^1 \ll N_s^0$ a magnetic field depopulates the upper subband completely and quantum Hall plateaus appear as usual at even integer filling factors (spin splitting is neglected). Here we define ν^i as the filling factor in subband i given by the carrier density in this subband, $\nu^i = N_s^i h/eB$. For larger values of $N_s^1 \leq N_s^0$ the carrier densities of both subbands can match at a given magnetic field and consequently both subbands have the same filling factor $\nu^0 = \nu^1$. In this case a quantum Hall plateau corresponding to $\nu = \nu^0 + \nu^1$ is observed provided ν is an integer. At an intermediate situation (between $N_s^1 \ll N_s^0$ and $N_s^1 \leq N_s^0$) the magnetic field is not strong enough to either depopulate the upper subband or to match the two carrier densities and ν^0 and ν^1 will not be an integer any more. Consequently the corresponding quantum Hall plateau will be suppressed. The subband structure of the parabolic well is calculated self-consistently by explicitly taking into account the influence of the magnetic field on the density of states. The resulting nonlinear Landau level fan diagram explains nicely the experimental observations.

The GaAs/$Al_xGa_{1-x}As$ parabolic quantum well is grown by molecular beam epitaxy and has the following sequence: on top of the substrate there is a 400 nm GaAs buffer layer, then 200 nm $Al_{0.3}Ga_{0.7}As$, 16 nm $Al_{0.3}Ga_{0.7}As$ with Si-doping ($N_D = 2.5 \times 10^{17}$ cm^{-3}), 20 nm $Al_{0.3}Ga_{0.7}As$ spacer, the 75 nm wide parabolic well with x varying $0 < x < 0.1$, 20 nm $Al_{0.3}Ga_{0.7}As$ spacer,

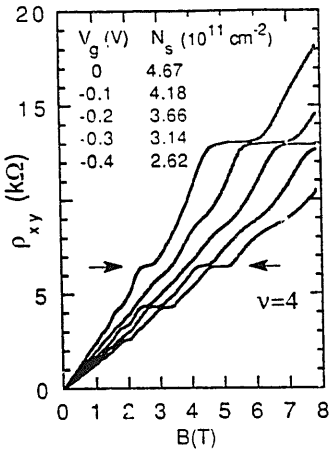

Fig. 1. Hall resistance ρ_{xy} for different carrier densities. The arrows indicate the $\nu = 4$ plateau which vanishes and reappears in this range of N_s.

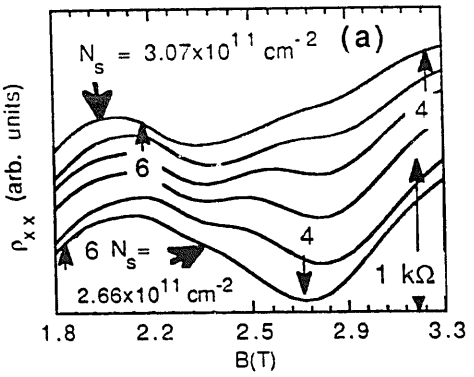

Fig. 2. Summary of ρ_{xx} measurements for a series of carrier densities. The curves are vertically offset for clarity. The vertical arrows indicate the position of filling factor $\nu = 4$ and $\nu = 6$ for the total carrier density.

and 101 nm Si-doped $Al_{0.3}Ga_{0.7}As$ ($N_D = 2.5 \times 10^{17}$ cm^{-3}). At 4.2 K the mobility of the electron gas in the well is $\mu = 100\,000$ cm^2/V s and the carrier density $N_s = 5 \times 10^{11}$ cm^{-2}. The mesa structure is a Hall geometry with a width of 50 μm and a spacing between the voltage probes of 150 μm. Ohmic contacts are made by alloying AuGe/Ni and a semi-transparent front gate (Ti/Au) is evaporated onto the sample. This allows us to tune the carrier density in the parabolic well and with it the width of the electron system and the number of occupied subbands [4]. The high quality of our sample and the reliability of the front gate are also demonstrated in far-infrared measurements [5]. The DC-transport measurements are performed in a superconducting magnet (0–10 T) and the sample is immersed in liquid helium at $T = 2.2$ K. The magnetic field is oriented perpendicular to the plane of the 2DEG. The samples are cooled down in the dark.

Fig. 1 presents a series of Hall measurements for five different carrier densities. For a large negative bias $V_g = -0.4$ V and consequently low carrier density $N_s = 2.62 \times 10^{11}$ cm^{-2} only one subband in this parabolic well is populated. The resulting Hall resistance ρ_{xy} shows clearly resolved Hall steps for filling factors $\nu = 4, 6, 8, 10$. For increasing carrier density, the plateau at $\nu = 4$ becomes weaker, vanishes and reappears again for large values of N_s. A similar behavior, but less strongly pronounced, is also observed for the $\nu = 6$ and $\nu = 8$ plateau.

For all the measurements the behavior of ρ_{xx} and ρ_{xy} is clearly correlated. In case of a suppressed Hall plateau in ρ_{xy}, there is only a weakly pronounced minimum or even none for the corresponding filling factor in ρ_{xx}. Since the magnetoresistance ρ_{xx} is more sensitive and shows more structure reflecting the actual density of states, we will concentrate our discussion on the data presented in fig. 2. For a series of carrier densities ρ_{xx} is plotted as a function of B. The curves are vertically offset with respect to each other for clarity. The range of magnetic fields is chosen so that the minima related to $\nu = 4$ and $\nu = 6$ dominate the spectrum. It is important to note that

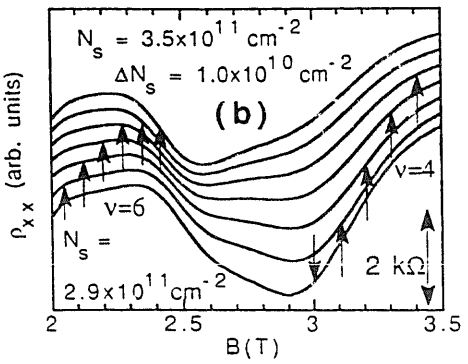

Fig. 3. Calculated magnetoresistance from a self-consistent calculation taking into account the magnetic field dependent density of states. Positions of total filling factor $\nu = 4$ are indicated by arrows. The overall agreement with the experimental data in fig. 2 is remarkably good.

the positions of the minima do not coincide with the filling factor ν related to the total carrier density of the sample. They can be related to the filling factors of the respective subbands. However, since the carrier densities of the various subbands oscillate as a function of B, the filling factor of a certain subband depends on the gate voltage V_g as well as on B. Thus, we will focus our discussion on the total filling factor ν being related to the total carrier density N_s, which does not depend on B. The way we determine N_s, proceeds as follows: Every time a well-defined Hall plateau occurs in ρ_{xy}, the position of the Fermi energy and thus the number of occupied Landau levels is unambiguous. In that case the corresponding minimum in ρ_{xx} occurs at a filling factor ν related to the total carrier density N_s. Repetition of this procedure for a series of V_g-values results in a smooth N_s versus V_g curve. This allows us to calculate the corresponding values of total N_s and total ν for a measurement at a given V_g even though the minima in ρ_{xx} might not correspond to integer values of ν. The interesting feature in fig. 2 is the position of $\nu = 4$ marked by the respective arrow with respect to the minima in ρ_{xx}. For low values of N_s the position of $\nu = 4$ is very close to a minimum. However, for high carrier densities, the arrow points to a maximum of ρ_{xx}. In agreement with the usual picture of the quantum Hall effect, which requires a pronounced minimum in ρ_{xx} for the occurrence of a Hall plateau, the Hall plateaus are suppressed in this range of carrier densities (see fig. 1). In addition there occurs a double minimum structure between $B = 2$ and 3 T corresponding to filling factors $4 < \nu < 6$. Here the influence of the higher subband becomes prominent and the interplay of the Landau levels of different subbands is directly reflected in ρ_{xx}. Correspondingly, the quantum Hall plateaus for $\nu = 6$ and $\nu = 8$ are destroyed in this range of magnetic fields (see fig. 1).

For a further understanding of this process, we solved self-consistently Poisson's and Schrödinger's equations in the presence of a magnetic field. All parameters for this calculation are given by the structure design. The Landau levels are modelled by a Gaussian density of states (DOS) with a FWHM of $\Gamma = 0.5\ \text{meV} \times (B[\text{T}])^{1/2}$ [6]. These parameters describe reasonably well previous magnetocapacitance measurements [7,8] on samples with similar mobilities. Consequently there are no adjustable parameters. We did not take into account complications such as spin splitting of the Landau levels, a constant background DOS [9], a filling factor dependent DOS or a subband dependent scattering time [10]. The results are not qualitatively changed by a further refined model of the DOS. In contrast to refs [8,11], it is not sufficient to model the magnetic field dependent DOS on top of a field-independent subband structure. For a typical sample, the electrical confinement energies are smaller, due to the width of well, and thus comparable to the cyclotron energy $\hbar\omega_c$ even at moderate magnetic fields. This leads to a considerable influence of the magnetic field on the subband energies as well as on the subband carrier densities making a simple fan chart invalid. The results of the self-consistent calculation are depicted in fig. 4 for $N_s = 5.0 \times 10^{11}\ \text{cm}^{-2}$. The upper most part (a) shows the carrier densities in the lowest three subbands as a function of magnetic field. All values of N_s^i depend strongly on B, and around $B = 5$ T, the two lowest subbands have almost the same amount of carriers. This situation corresponds to $\nu = 4 = \nu^1 + \nu^2 = 2 + 2$ and therefore the reappearance of the corresponding quantum Hall plateau. The lowest part of fig. 4 shows the calculated Landau level fan diagram and the corresponding Fermi energy. The energies are plotted so that the Landau levels belonging to the lowest subband $\langle 0 | j \rangle$ are linear. Consequently the Landau levels of the upper subband are highly nonlinear. A better way of plotting the same data is presented in the middle part of fig. 4. The reference energy in this case is the Fermi energy which is chosen to be $E_F = 0$. The dashed lines indicate the Landau levels and the solid lines the subband energies. A Landau level of a subband is populated when it crosses the subband energy. It is obvious that the subband separation $E_1 - E_0 = E_{\langle 1|j\rangle} - E_{\langle 0|j\rangle}$ depends on B and influences strongly the population of the various subbands.

To compare our experimental results more closely with the calculation we evaluated directly

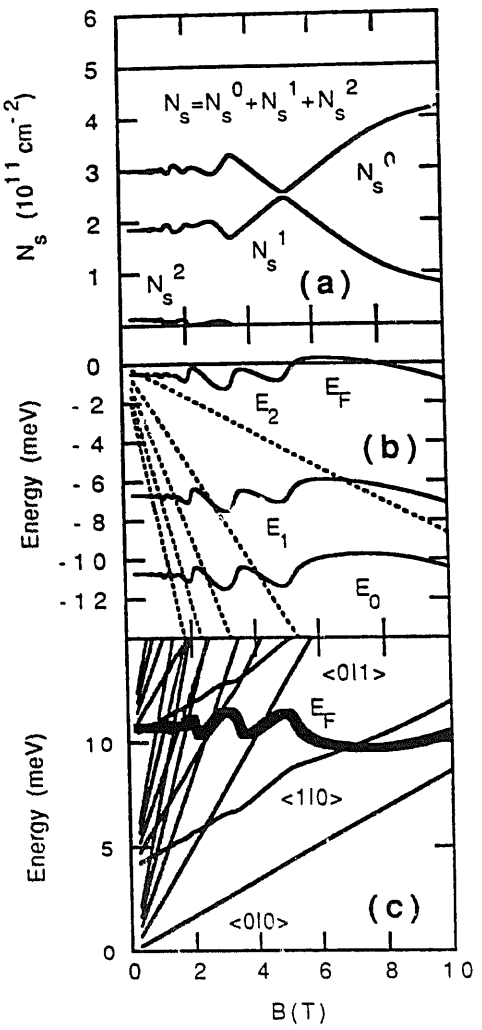

Fig. 4. Calculated subband carrier densities (a) and subband energies (b+c) as a function of B. The carrier density in subband i is denoted by N_S^i, the corresponding subband energy by E_i. A Landau level j of subband i, denoted by $\langle i|j\rangle$, is populated if it is below the Fermi level in (c), or, in (b), if the Landau level j is below the subband energy j.

ρ_{xx}. From the DOS we can calculate the magnetic field dependent conductivity $\sigma_{xx}(B)$ [6,11]. Since the Hall resistance behaves almost classical in the regime of interest due to the suppression of the Hall plateaus, it is reasonable to assume $\sigma_{xy} = -eN_s/B$ for the Hall conductivity. This allows us to calculate $\rho_{xx}(B)$ as presented in fig. 3b. Again the curves are vertically offset with respect to each other for clarity. The range of carrier densities presented here differs slightly (less than 10%) from fig. 2, because the detailed population behavior of the upper subband is a complicated process which depends on the particular form of the exchange-correlation potential. For a detailed discussion see ref. [8]. Nevertheless, this is expected to be a small effect and does not change the overall understanding of the experiment. The position of $\nu = 4$ with respect to the minima in ρ_{xx} as well as the N_s-independent position of the minima for intermediate carrier densities around $B = 2.5$ T are very well reproduced by the calculation. Even the double minimum structure at 2.2 T $< B <$ 2.9 T is clearly visible in the theoretical results. However, the detailed curvature of the ρ_{xx}-measurement as well as the height of the maxima in ρ_{xx} is very sensitive to the actual DOS, which was only approximated in the present calculation. Nevertheless, there is a good understanding of the overall behavior of ρ_{xx} and correspondingly of ρ_{xy}. The calculation shows, that even for a sample with infinite mobility at very low temperatures (delta function shaped Landau levels) there is a regime, where the position of $\nu = 4$ lies in a maximum of ρ_{xx}. Consequently, the $\nu = 4$ Hall plateau cannot be recovered by lowering the temperature of the measurement. The suppression and recovery of the quantum Hall plateaus is a direct consequence of the subband structure in a parabolic well, which is influenced by the magnetic field.

Our results relate previous experiments on heterostructures with two occupied subbands [12] and wide parabolic wells [2] where the disappearance of even integer quantum Hall Plateaus was reported. The suppression of quantum Hall states depends sensitively on the subband structure of the respective sample.

In conclusion, we have observed the suppression and recovery of quantum Hall plateaus in a parabolic quantum well. This phenomenon is explained by the magnetic-field-dependent density of states, which directly influences the subband structure in a parabolic well in the case of multiple subband occupancy.

We thank H. Kroemer, S. Sasa, P. Hopkins and B. Gwinn for stimulating discussions. This work was supported by the Air Force and "QUEST", a National Science Foundation Science and Technology Center.

References

[1] For a review, see The Quantum Hall Effect, eds. R.E. Prange and S.M. York (1987).

[2] E.G. Gwinn, R.M. Westervelt, P.F. Hopkins, A.J. Rimberg, M. Sundaram, and A.C. Gossard, Phys. Rev. B 39 (1989) 6260.

[3] T. Sajoto, J. Jo, M. Santos and M. Shayegan, Appl. Phys. Lett. 55 (1989) 1430.

[4] A. Wixforth, M. Sundaram, K. Ensslin, J.H. English and A.C. Gossard, Appl. Phys. Lett. 56 (1990) 454.

[5] A. Wixforth, M. Sundaram, K. Ensslin, J.H. English and A.C. Gossard, Surf. Sci. 267 (1992) p. 523.

[6] R.R. Gerhardts, Surf. Sci. 58 (1976) 227.

[7] D. Weiss, V. Moser, V. Gudmundsson, R.R. Gerhardts and K. von Klitzing, Solid State Commun. 62 (1987) 89.

[8] K. Ensslin, D. Heitmann, R.R. Gerhardts and K. Ploog, Phys. Rev. B 39 (1989) 12993.

[9] See for example E. Gornik, R. Lassnig, G. Strasser, H.L. Störmer, A.C. Gossard and W. Wiegmann, Phys. Rev. Lett. 54 (1985) 1820.

[10] See for example K. Ensslin, D. Heitmann and K. Ploog, Phys. Rev. B 37 (1988) 10150.

[11] G. Gobsch, D. Schulze and G. Paasch, Phys. Rev. B 38 (1988) 10943.

[12] Y. Guldner, J.P. Vieren, M. Voos, F. DeLahaye, D. Dominguez, J.P. Hirtz and M. Razeghi, Phys. Rev. B 33 (1986) 3990.